Adipocyte-Specific *Hnrnpa1* Knockout Aggravates Obesity-Induced Metabolic Dysfunction via Upregulation of CCL2

Xiaoya Li, Yingying Su, Yiting Xu, Tingting Hu, Xuhong Lu, Jingjing Sun, Wenfei Li, Jian Zhou, Xiaojing Ma, Ying Yang, and Yuqian Bao

Diabetes 2024;73:713–727 | https://doi.org/10.2337/db23-0609

Heterogeneous nuclear ribonucleoprotein A1 (HNRNPA1) is involved in lipid and glucose metabolism via mRNA processing. However, whether and how HNRNPA1 alters adipocyte function in obesity remain obscure. Here, we found that the obese state downregulated HNRNPA1 expression in white adipose tissue (WAT). The depletion of adipocyte HNRNPA1 promoted markedly increased macrophage infiltration and expression of proinflammatory and fibrosis genes in WAT of obese mice, eventually leading to exacerbated insulin sensitivity, glucose tolerance, and hepatic steatosis. Mechanistically, HNRNPA1 interacted with Ccl2 and regulated its mRNA stability. Intraperitoneal injection of CCL2-CCR2 signaling antagonist improved adipose tissue inflammation and systemic glucose homeostasis. Furthermore, HNRNPA1 expression in human WAT was negatively correlated with BMI, fat percentage, and subcutaneous fat area. Among individuals with 1-year metabolic surgery follow-up, HNRNPA1 expression was positively related to percentage of total weight loss. These findings identify adipocyte HNRNPA1 as a link between adipose tissue inflammation and systemic metabolic homeostasis, which might be a promising therapeutic target for obesity-related disorders.

ARTICLE HIGHLIGHTS

- Heterogeneous nuclear ribonucleoprotein A1 (HNRNPA1) is decreased during obesity, but the specific role in adipose tissue remains unclear.
- Adipocyte-specific depletion of *Hnrnpa1* accelerates adipose tissue inflammation and systemic metabolic disorders via enhancing mRNA stability of chemokine CCL2.
- CCL2 receptor antagonist rescues metabolic dysfunction elicited by *Hnrnpa1* depletion.
- HNRNPA1 expression in human adipose tissue is closely related to BMI, fat percentage, and subcutaneous fat area and is positively associated with percentage of total weight loss 1 year after bariatric surgery.

In past decades, the prevalence of obesity worldwide has risen dramatically (1). Obesity-related metabolic disorders (insulin resistance, type 2 diabetes, and cardiovascular disease) represent a severe health issue. The critical characteristic of obesity is chronic low-grade inflammation and metabolic disorders (2). Adipose tissue is now recognized as a critical metabolic organ that regulates whole-body energy homeostasis via the regulation of energy storage and dissipation (3) and secretion of adipokines (4). During obesity, increased proinflammatory adipokines activate the immune system and drive it toward a proinflammatory phenotype (5). Among the adipokines, immune-modulating adipokines, such as interleukin-6 (IL-6), IL-8, C-X-C motif chemokine ligand 5, and C-C motif chemokine ligand 2 (CCL2, also known as MCP-1), play important roles in adipose tissue macrophage (ATM) recruitment and activation (6), resulting in a feedback loop of adipose tissue inflammation. Recently, many of these inflammatory signals generated by adipose tissue were reported to block insulin sensitivity that finally

Department of Endocrinology and Metabolism, Shanghai Diabetes Institute, Shanghai Clinical Center for Diabetes, Shanghai Key Laboratory of Diabetes Mellitus, Shanghai Key Clinical Center for Metabolic Disease, Shanghai Jiao Tong University School of Medicine Affiliated Sixth People's Hospital, Shanghai, China

Corresponding authors: Yuqian Bao, yqbao@sjtu.edu.cn, Ying Yang, yangyingsh@sjtu.edu.cn, and Xiaojing Ma, maxiaojing@sjtu.edu.cn

Received 1 August 2023 and accepted 28 January 2024

This article contains supplementary material online at https://doi.org/10.2337/figshare.25137425.

X.Li, Y.S., and Y.X. contributed equally to this work.

resulted in systemic metabolic dysfunction (7,8). Although extensive research and several mechanisms have been proposed, the causal processes promoting adipose tissue inflammation in obesity are continuously being expanded and have always been a hot spot for research (9).

It is well established that many different types of RNA-binding proteins exist in eukaryotic cells. RNA-binding proteins could combine with specific sequences or secondary structures of mRNA transcript variants to regulate their synthesis, expression, and function (10). A growing amount of research indicates that RNA processing prepares the transcript so that it can function in adipogenesis (11), adipocyte lipolysis (12), adipocyte thermogenesis (13), etc. Heterogeneous nuclear ribonucleoprotein A1 (HNRNPA1), a ubiquitously expressed member of the HNRNP family of RNA-binding proteins, contains highly conserved RNA recognition domains and a nuclear targeting sequence (14). It takes part in multiple cell functions, including regulation of transcription factors, alternative splicing, mRNA stability, mRNA nuclear export, and miRNA processing (15). Emerging evidence indicates that HNRNPA1 plays important roles in regulating metabolic balance in the liver and muscle through multiple target genes (16–18). However, it remains unclear whether HNRNPA1 in adipose tissue would exert any effect on metabolic disorders. In this study, we comprehensively investigated the role of HNRNPA1 in adipose tissue inflammation and obesity-related metabolic disorders and deciphered its mechanisms via regulating mRNA stability of CCL2, which could provide therapeutic strategies against obesity and metabolic diseases.

RESEARCH DESIGN AND METHODS

Animal Experiments

Hnrnpa1 flox/flox (fl/fl) C57BL/6J mice were purchased from GemPharmatech Co. Ltd., in which exons 2–11 of the *Hnrnpa1* allele were flanked by *loxP* site. Adipoq-Cre C57BL/6J mice were purchased from The Jackson Laboratory. Adipocyte-specific *Hnrnpa1* knockout (*Hnrnpa1* ako) mice were generated by intercrossing *Hnrnpa1* fl/fl mice with heterozygous adipoq-Cre mice. *Hnrnpa1* ako mice were genotyped by PCR using DNA isolated from tails. The genotyping primers are shown in Supplementary Table 1. Detailed procedures for mouse modeling, metabolic phenotype, and serum analysis can be found in the Supplementary Methods.

Histological, Immunohistochemistry, and Immunofluorescence Analysis

For tissue staining, dissected adipose and liver tissues were fixed in 4% paraformaldehyde (G1101; Servicebio) and embedded by paraffin. Tissue sections were stained with hematoxylin-eosin (H-E) (G1076; Servicebio) or antibodies, including anti-F4/80 and anti-CD11c, followed by species-specific secondary antibodies. The images were acquired by a microscope (Leica) using a 20× objective.

Cell Culture, Differentiation, and Treatment

The mouse stromal vascular fraction (SVF) was isolated from the included inguinal white adipose tissue (iWAT) depot of 4–6-week-old male mice. Detailed steps for cell isolation, culture, and differentiation are presented in the Supplementary Material, and mature adipocytes were used for further studies. Adipoq-Cre adenovirus (Cre AdV) and negative control were provided by Genechem Co. Ltd., which were used to knockdown *Hnrnpa1* in primary adipocytes from *Hnrnpa1* fl/fl mice.

To assess the insulin-induced AKT pathway, primary adipocytes were stimulated with insulin (10 nmol/L for 10 min). The glucose uptake ability of adipocytes was measured using the Glucose Uptake-Glo Assay Kit (J1342; Promega). For lipolysis assay, adipocytes were stimulated with tumor necrosis factor-α (TNF-α) (10 ng/mL). The Mouse CCL2/JE/MCP-1 Quantikine ELISA Kit (MJE00B; R&D Systems) was used to analyze the level of CCL2 according to the instructions provided in the manual. To assess the mRNA stability of CCL2 under HNRNPA1 knockdown, differentiated 3T3-L1 cells were treated with 5 μg/mL actinomycin D (HY-17559; MedChemExpress) and harvested at indicated time points.

Lentivirus-Mediated Gene Transfer

pLKO.1-puro empty vector plasmid, HNRNPA1 shRNA plasmids, pSLenti-CMV-7Myc-EGFP-PGK-Puro-WPRE empty vector plasmid, pSLenti-CMV-7Myc-Slc2a4-linker-EGFP-PGK-Puro-WPRE plasmid, psPAX2, and pMD2.G were used for the lentiviral package. The procedure of lentivirus package, concentration, and shRNA sequences are shown in the Supplementary Methods.

Human Adipose Tissue Samples

There were 236 individuals included for adipose HNRNPA1 mRNA expression analysis. These individuals underwent either elective abdominal surgery for cholecystectomy or weight reduction bariatric surgery at Shanghai Jiao Tong University School of Medicine Affiliated Sixth People's Hospital between July 2019 and August 2020. Detailed standards about recruitment, exclusion, clinical data, and sample acquisition were described previously (19). The human study was approved by the ethics committee of Shanghai Jiao Tong University School of Medicine Affiliated Sixth People's Hospital.

RNA Immunoprecipitation Assay

According to the manufacturer's instructions, the RNA immunoprecipitation (RIP) assay was performed using Magna RIP RNA-Binding Protein Immunoprecipitation Kit (17-700; Millipore). Detailed steps are provided in the Supplementary Material.

Western Blot Analysis

Tissue and cell samples were lysed with radioimmunoprecipitation assay lysis buffer containing EDTA-free protease and phosphatase inhibitor cocktail. Detailed steps are provided in the Supplementary Material.

RNA Extraction, Quantitative RT-PCR, and RNA Sequencing

Total RNA was extracted from cells and tissues using TRIzol reagent (15596018; Invitrogen). A total of 500 ng RNA was reversed to cDNA using the PrimeScript RT Reagent Kit with gDNA Eraser (RR047B; Takara Bio) according to the manufacturer's instructions. Quantitative RT-PCR (RT-qPCR) was performed using SYBR qPCR Master Mix (R222; Vazyme) on a Bio-Rad C1000 thermal cycler. Experiments were repeated three times. Primers for RT-qPCR are listed in Supplementary Table 2.

For RNA sequencing (RNA-seq), total RNA samples of primary adipocytes and iWAT from *Hnrnpa1* fl/fl and ako mice were extracted using TRIzol reagent. The specific sequencing procedure is shown in the Supplementary Methods.

Quantification and Statistical Analysis

All data are presented as mean ± SEM, median (interquartile range), and *n* (%). Statistical analysis was performed using unpaired two-tailed Student *t* test or two-way ANOVA with Šidák multiple comparisons test. Correlational analyses were conducted by nonparametric Spearman correlation. ImageJ version 1.53 software was used for Western blot image densitometry analysis.

Data and Resource Availability

The data sets generated and/or analyzed during the current study are available from the corresponding authors upon reasonable request.

RESULTS

HNRNPA1 Expression in Adipose Tissue Decreased in Obesity

We analyzed HNRNPA1 expression in human metabolic tissues and found that its expression was much more abundant in WAT than liver, muscle, pancreas, and hypothalamus based on the Genotype-Tissue Expression (GTEx) database (20) (Supplementary Fig. 1). We therefore measured HNRNPA1 expression in human subcutaneous adipose tissue (SAT) and visceral adipose tissue (VAT) from 10 nonobese and 10 obese individuals. Representative expression and quantitative analysis showed an obvious reduction in HNRNPA1 protein levels among obese humans compared with the control subjects (Fig. 1*A* and *B*). Moreover, weight loss caused by bariatric surgery upregulated mRNA levels of HNRNPA1 in human SAT according to the data set from Poitou et al. (21) (Fig. 1*F*).

In addition, high-fat diet (HFD) feeding resulted in decreased mRNA and protein expression of HNRNPA1 in mouse iWAT and epididymal WAT (eWAT), while this effect was not observed in brown adipose tissue (BAT) (Fig. 1*D*–*F*). These data suggest that obesity status could downregulate HNRNPA1 expression of adipose tissue.

Adipocyte-Specific HNRNPA1 Deletion Exacerbates Systemic Metabolic Deterioration

The specific role of HNRNPA1 in adipose tissue was investigated by crossing *Hnrnpa1* fl/fl mice with adipoq-Cre mice (Fig. 2*A*). As expected, HNRNPA1 was significantly reduced in adipose tissues, while there was no change in mRNA and protein levels in the hypothalamus, liver, and muscle (Fig. 2*B*–*D*), verifying the specificity of the *Hnrnpa1* ako mice. After isolating SVF and mature adipocyte fraction, Western blot experiments provided further evidence for adipocyte-specific knockout of *Hnrnpa1* (Supplementary Fig. 2). We first observed the phenotypes in the setting of normal chow diet (NCD) feeding for 16 weeks. The body weight, tissue weight, and food intake of *Hnrnpa1* ako mice were comparable with the control group (Supplementary Fig. 3*A*–*C*). There was also no difference in glucose tolerance and insulin sensitivity (Fig. 2*E* and *F*). However, pyruvate tolerance test analysis showed that blood glucose levels were mildly higher in *Hnrnpa1* ako mice than in *Hnrnpa1* fl/fl, indicating impaired pyruvate tolerance (Fig. 2*G*).

To further investigate the functional significance of adipocyte-specific *Hnrnpa1* deletion, mice were fed a 60% HFD for 20 weeks, starting at 8 weeks of age. Both *Hnrnpa1* fl/fl and *Hnrnpa1* ako mice showed a similar age-dependent increase in body weight (Fig. 3*A*). Besides, the food intake (Fig. 3*B*), fat mass, and lean mass showed no difference (Fig. 3*C*). Remarkably, *Hnrnpa1* ako mice displayed significantly impaired glucose intolerance and insulin sensitivity (Fig. 3*D* and *E*). For a better understanding of the role of HNRNPA1 in insulin action, we harvested adipose, liver, and muscle tissue after 10 min of intraperitoneal insulin injection. Consistent with the insulin tolerance studies, insulin-stimulated AKT phosphorylation was significantly lower in iWAT, eWAT, and liver but not in muscle tissues of *Hnrnpa1* ako versus *Hnrnpa1* fl/fl mice (Fig. 3*F*). The ability of insulin to suppress lipolysis also indicated insulin sensitivity of adipose tissue, and we found that hormone-sensitive lipase phosphorylation inhibition and serum free fatty acid suppression were both impaired in *Hnrnpa1* ako mice (Fig. 3*G* and *H*).

In addition, we examined the impact of HNRNPA1 on liver metabolism under HFD feeding. *Hnrnpa1* ako mice showed significantly higher levels of glycemia than control mice during pyruvate tolerance testing (Fig. 3*I*), indicating overactivated hepatic gluconeogenesis. We analyzed mouse liver tissues for the key gluconeogenic gene expression and found that Pepck and G6pc were expressed higher in the liver of *Hnrnpa1* ako mice (Fig. 3*J*). The liver showed a light gray color, and H-E staining demonstrated increased lipid accumulation in *Hnrnpa1* ako mice (Fig. 3*K* and *L*), indicating that adipocyte HNRNPA1 deletion promoted hepatic steatosis. Consistently, hepatic triglyceride levels were significantly increased (Fig. 3*M*). Overall, the data demonstrated that adipocyte HNRNPA1 plays important roles in metabolic disorders.

HNRNPA1 Deficiency Aggravates Adipose Inflammation

Even though no obvious changes in global metabolic phenotypes were observed in the NCD-fed mice between

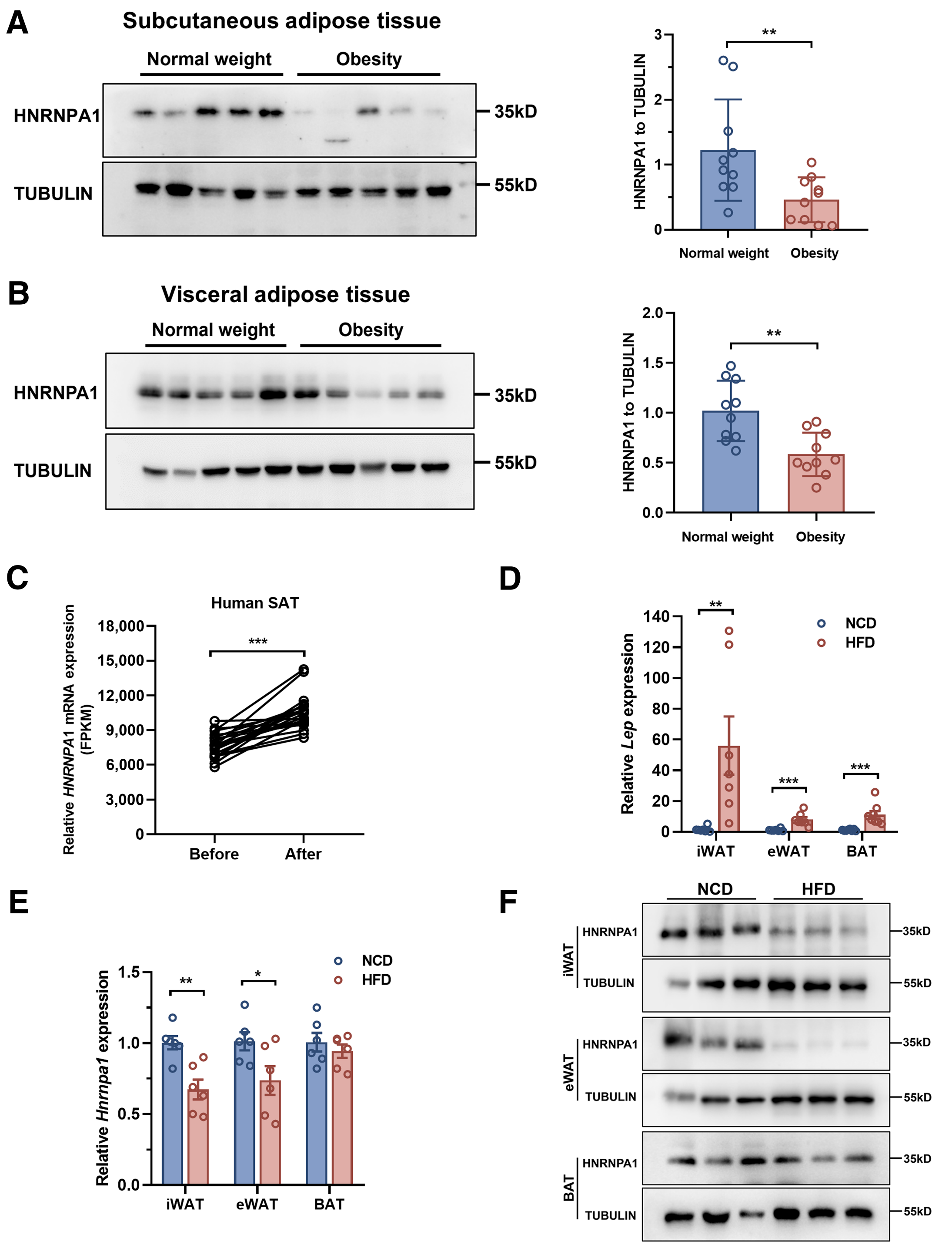

Figure 1—HNRNPA1 expression in adipose tissue decreases in obesity. *A*: Representative Western blot analysis and quantification of HNRNPA1 expression in SAT from normal weight and obese individuals (n = 10 biologically independent samples). *B*: Representative Western blot analysis and quantification of HNRNPA1 expression in VAT from normal weight and obese individuals (n = 10 biologically independent samples). *C*: Changes of *HNRNPA1* mRNA expression levels in human SAT before and after 3 months of Roux-en-Y gastric bypass. *D* and *E*: RT-qPCR analysis of leptin and *Hnrnpa1* mRNA expression in iWAT, eWAT, and brown adipose tissue (BAT) from NCD- or HFD-fed mice (n = 6 biologically independent mice). *F*: Representative Western blot analysis of HNRNPA1 expression in iWAT, eWAT, and BAT from NCD- and HFD-fed mice (n = 3 biologically independent samples per group). Data are mean ± SEM. *P* values were determined by two-tailed Student *t* test. *$P < 0.05$, **$P < 0.01$, ***$P < 0.001$.

genotypes, we found that *Hnrnpa1* ako mice showed elevated proinflammatory gene expression and a trend toward decreased expression of anti-inflammatory genes in WAT (Fig. 4*A* and *B*), while no differences were observed in adipogenesis, lipolysis, and glucose metabolism genes in WAT between *Hnrnpa1* fl/fl and *Hnrnpa1* ako mice

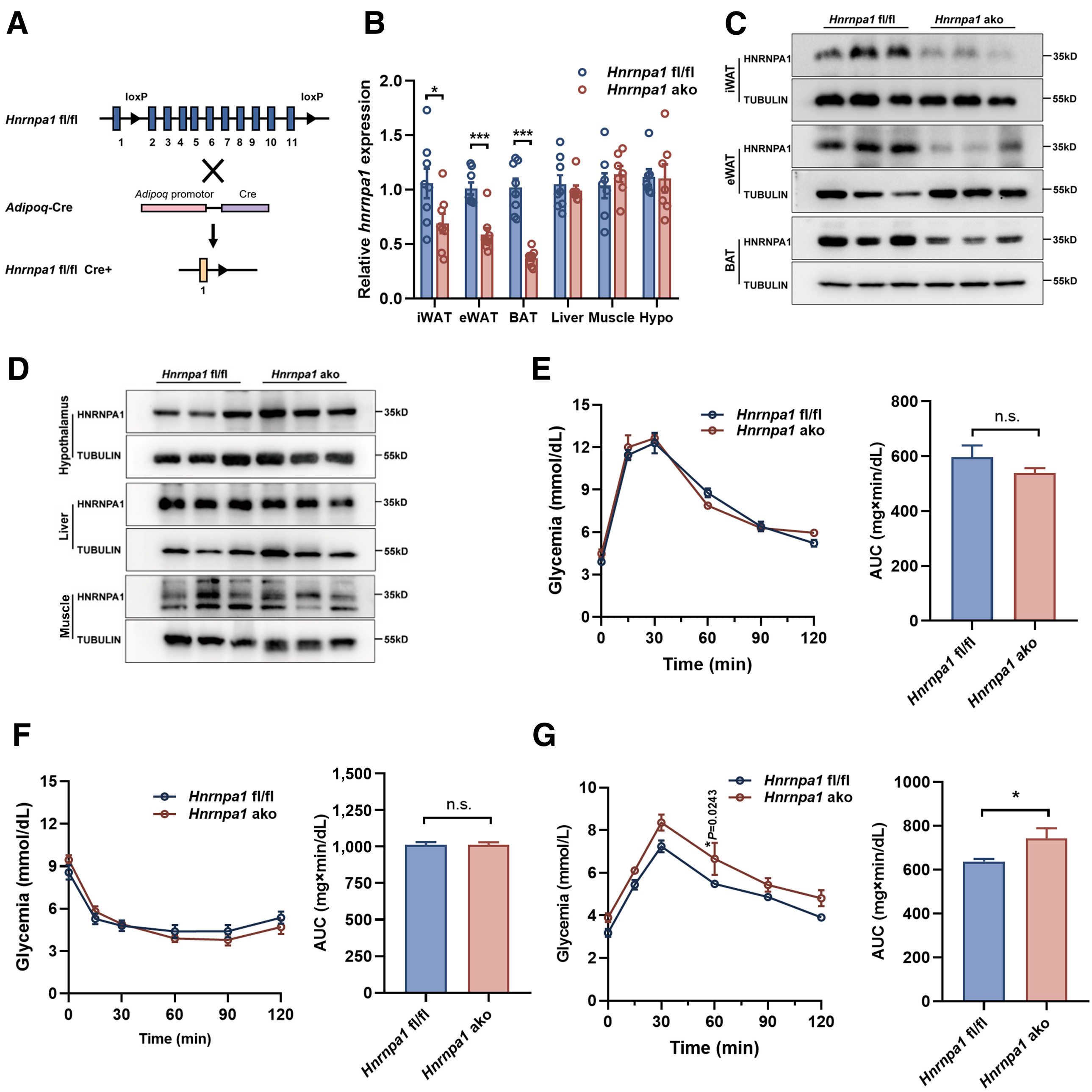

Figure 2—Adipocyte HNRNPA1 abrogation promotes hepatic gluconeogenesis under NCD feeding. *A*: Schematic representation of the generation of the *Hnrnpa1* ako mouse model. *B*: RT-qPCR analysis of *Hnrnpa1* mRNA expression in iWAT, eWAT, brown adipose tissue (BAT), liver, muscle, and hypothalamus (Hypo) from *Hnrnpa1* fl/fl or *Hnrnpa1* ako mice (*n* = 6 biologically independent mice). *C*: Representative Western blot analysis of HNRNPA1 expression in iWAT, eWAT, and BAT from *Hnrnpa1* fl/fl or *Hnrnpa1* ako mice (*n* = 3 biologically independent mice). *D*: Representative Western blot analysis of HNRNPA1 expression in hypothalamus, liver, and muscle (*n* = 3 biologically independent samples per group). *E*: Glucose tolerance test and area under the curve (AUC) of *Hnrnpa1* fl/fl or *Hnrnpa1* ako mice (*n* = 5 biologically independent mice). *F*: Insulin tolerance test and AUC of *Hnrnpa1* fl/fl or *Hnrnpa1* ako mice (*n* = 5 biologically independent mice). *G*: Pyruvate tolerance test and AUC of *Hnrnpa1* fl/fl or *Hnrnpa1* ako mice (*n* = 5 biologically independent mice). Data are mean ± SEM. *P* values were determined by unpaired two-tailed Student *t* test (*B*) or two-way ANOVA with Šidák multiple comparisons test (*E*, *F*, and *G*). $^*P < 0.05$, $^{***}P < 0.001$.

(Supplementary Fig. 3*D* and *E*). Since adipose tissue inflammation is known to promote lipolysis (22), we also detected a significant increase in lipolysis of *Hnrnpa1* ako mice whether at room temperature or under cold stimulation (Supplementary Fig. 3*F* and *G*).

Moreover, in obese mice, we observed increased proinflammatory and decreased anti-inflammatory gene expression in WAT of *Hnrnpa1* ako mice (Fig. 4*C* and *D*). Previous studies reported that ATMs mainly accumulate in obese WAT, forming crown-like structures and leading

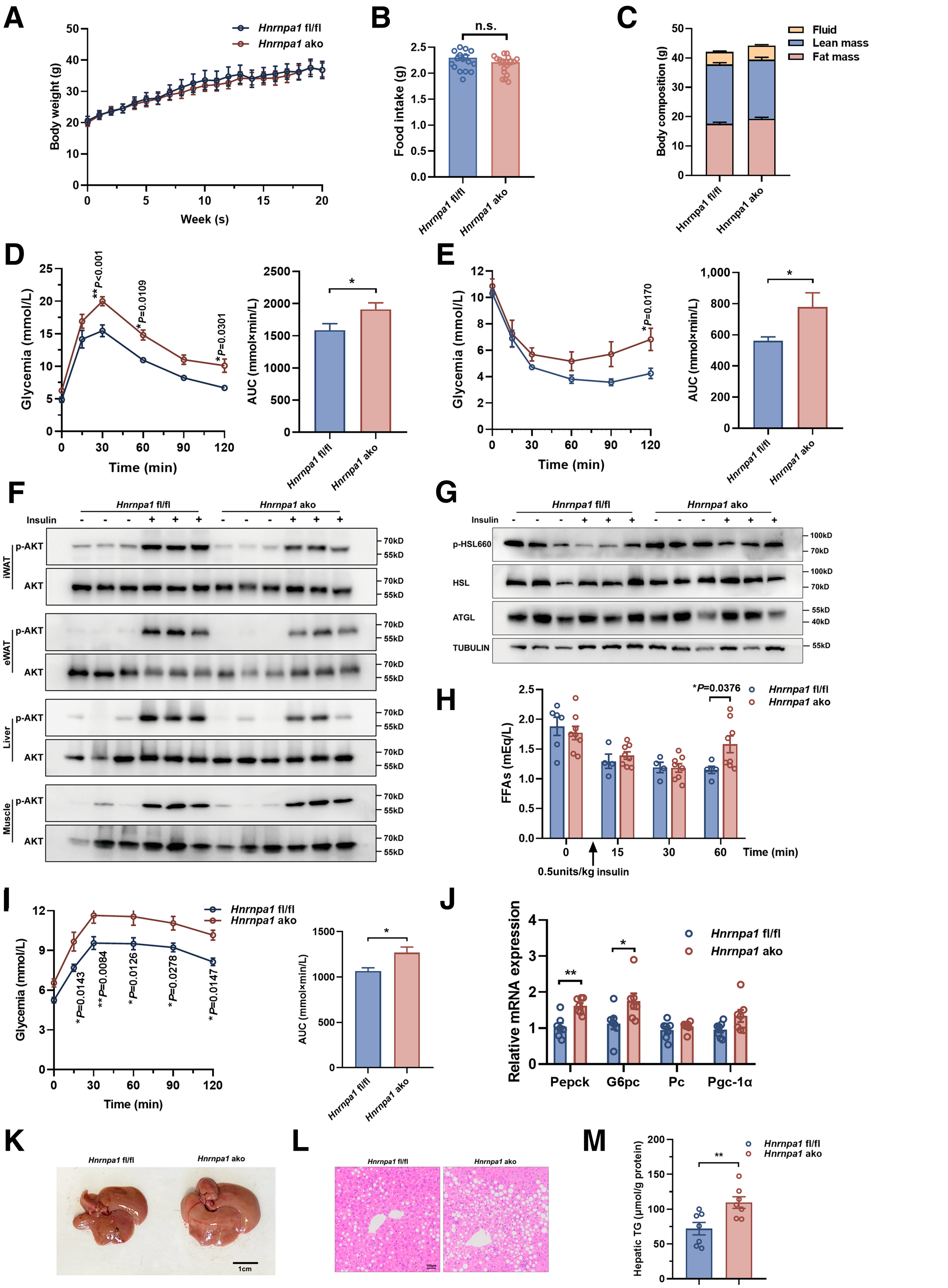

Figure 3—*Hnrnpa1* ako mice show metabolic impairments when maintained on an HFD. Male *Hnrnpa1* fl/fl and age-matched *Hnrnpa1* ako littermates were fed an HFD for 20 weeks, and HFD feeding started at 8 weeks of age. *A* and *B*: Body weight and food intake (*n* = 7 biologically independent mice). *C*: Body composition, including fat mass, lean mass, and fluid (*n* = 7 biologically independent mice). *D*: Glucose tolerance test and area under the curve (AUC) (*n* = 7 biologically independent mice). *E*: Insulin tolerance test and AUC (*n* = 7 biologically independent mice). *F*: Representative Western blot analysis of AKT phosphorylation in murine iWAT, eWAT, liver, and muscle after insulin administration (1 unit/kg) or PBS in vivo. *G*: Representative Western blot analysis of hormone-sensitive lipase (HSL)

to the development of chronic inflammation (23). Accordingly, we found a higher number of crown-like structures measured by F4/80 immunohistochemical staining in iWAT and eWAT from *Hnrnpa1* ako mice than *Hnrnpa1* fl/fl mice (Fig. 4*E*). CD11c is a classical marker of proinflammatory macrophages (24). Consistently, the intensity of CD11c staining in iWAT and eWAT was elevated in *Hnrnpa1* ako mice (Fig. 4*F* and G and Supplementary Fig. 4). As accumulative macrophage infiltration leads to adipocyte death and eventual fibrosis (25), *Hnnrpa1* ako mice showed increased expression of fibrotic genes in WAT (Supplementary Fig. 5), accelerating pathological remodeling of adipose tissue. Furthermore, *Hnrnpa1* ako mice showed high serum levels of inflammatory factors, including IL-1α, IL-9, IL-12p40, interferon-γ (IFN-γ), CCL2, TNF-α, MIP-1β, and granulocyte colony-stimulating factor (Fig. 4*H*). Additionally, we quantified immune cells using the FACS technique. SVFs were isolated from obese mice after 12 weeks of HFD feeding. The F4/80$^+$CD11b$^+$ cell numbers in iWAT and eWAT, as measured by FACS, were significantly higher in *Hnrnpa1* ako mice (Supplementary Fig. 6*A* and *B*). Taken together, these data suggest that adipocyte-specific *Hnrnpa1* knockout leads to increased adipose tissue inflammation.

HNRNPA1 Knockdown Exacerbates Adipocyte Function

A previous study reported that silencing of HNRNPA1 impaired insulin sensitivity in C2C12 myotubes (26). Thus, we explored whether the deletion of HNRNPA1 could affect adipocyte function. The SVF from the iWAT of *Hnrnpa1* fl/fl mice was harvested, and the differentiated adipocytes were infected with control or AdV. As expected, Cre AdV infection caused the knockdown of HNRNPA1 in primary adipocytes (Fig. 5*A*). HNRNPA1 knockdown did not affect the expression of genes involved in differentiation (*Adipoq*, *Fabp4*), lipolysis (*Lipe*, *Pnpla2*), and glucose metabolism (*Slc2a1*, *Slc2a4*) (Fig. 5*B*). Notably, HNRNPA1 knockdown impaired insulin-stimulated AKT phosphorylation, indicating impaired insulin signaling pathway (Fig. 5*C*). As insulin-AKT signaling stimulates glucose uptake via GLUT4 plasma membrane translocation (27), the immunofluorescence analysis showed that insulin-stimulated GLUT4 plasma membrane translocation was obviously decreased in HNRNPA1 knockdown adipocytes as visualized using confocal microscopy (Fig. 5*D*). The impaired ability of glucose uptake was also determined (Fig. 5*E*). Additionally, HNRNPA1 knockdown induced adipocyte lipolysis (Fig. 5*F* and *G*). These findings were consistent with the results in *Hnrnpa1* ako mice under HFD feeding, which further demonstrated that HNRNPA1 deficiency destroyed adipocyte function.

HNRNPA1 Deficiency Increases mRNA Stability of CCL2

To dissect the molecular mechanism of HNRNPA1 in adipose tissue, we examined the transcriptional profiles of iWAT from *Hnrnpa1* fl/fl and *Hnrnpa1* ako mice by performing RNA-seq analysis. Principal component analysis showed that iWAT from *Hnrnpa1* ako mice was separated from the control group (Fig. 6*A*). The pathway enrichment data showed that differential genes mainly enriched in cytokine-cytokine receptor interaction and chemokine signaling pathways (Fig. 6*B*). From the volcano plot, chemokines (including Ccl2, Ccl3, Ccl8, Ccl9, Cxcl10, and Cxcl13) were increased in the iWAT of *Hnrnpa1* ako mice (Fig. 6*C*). Then, we verified the expression of chemokines in primary adipocytes and found that there was a significant difference in Ccl2 expression between control and HNRNPA1 knockdown adipocytes (Fig. 6*D*). Besides, shRNA was used to knockdown *Hnrnpa1* mRNA in 3T3-L1 cells (Supplementary Fig. 7*A* and *B*), and decreased Ccl2 expression was also identified in *Hnrnpa1* knockdown cells (Fig. 6*E*). After knocking down *Hnrnpa1* in primary adipocytes, the secretion of CCL2 in the cell culture supernatant was also reduced (Supplementary Fig. 8). From these results, we conclude that HNRNPA1 deletion resulted in increased expression and secretion of CCL2.

HNRNPA1 is an RNA-binding protein that has been reported to be critical for mRNA processing (15). Therefore, to decipher the exact regulatory mechanism of HNRNPA1, RIP assay was performed, and the results suggested that HNRNPA1 could interact with Ccl2 mRNA (Fig. 6*F* and *G*). Importantly, HNRNPA1 knockdown increased the mRNA stability of Ccl2 in 3T3-L1 cells treated with actinomycin D (a specific RNA synthesis inhibitor) (Fig. 6*H*), which indicated that HNRNPA1 functioned via binding to mRNA of Ccl2 to inhibit its mRNA stability. Furthermore, we performed RNA-seq of mouse primary adipocytes derived from iWAT of *Hnrnpa1* fl/fl mice infected with control or Cre AdV, separately. The differentially expressed genes are shown in Supplementary Table 3, which included 66 upregulated genes and 122 downregulated genes (absolute $\log_2$ |fold change| ≥0.58, $P < 0.05$). Although other differentially expressed genes were identified, CCL2 was still one of the top differentially downregulated genes.

CCL2-CCR2 Signaling Antagonist Improves Metabolic Disorders of *Hnrnpa1* ako Mice Under HFD Feeding

Since CCL2 functioned mainly through CCR2 (28), several studies explored the role of the CCL2-CCR2 pathway in metabolic complications based on CCL2-neutralized antibody or antagonist (29,30). Thus, we aimed to detect whether CCL2-CCR2 signaling antagonist could rescue the metabolic

phosphorylation in murine iWAT after insulin administration (1 unit/kg) or PBS in vivo. *H*: Serum free fatty acid (FFA) levels of mice after insulin administration (0.5 units/kg) or PBS in vivo. *I*: Pyruvate tolerance test and AUC. *J*: RT-qPCR analysis of gluconeogenesis gene expression in liver (*n* = 7 biologically independent mice). *K*: Representative pictures of livers from *Hnrnpa1* fl/fl and *Hnrnpa1* ako mice. *L*: Representative images of H-E–stained liver tissues (*n* = 4 per group; scale bar = 100 μm). *M*: Hepatic triglyceride (TG) levels (*n* = 7 for each group). Data are mean ± SEM. *P* values were determined by unpaired two-tailed Student *t* test (*A*–*C*, *J*, and *M*) or two-way ANOVA with Šidák multiple comparisons test (*D*, *E*, *H*, and *I*). *$P < 0.05$, **$P < 0.01$. ATGL, adipose triglyceride lipase.

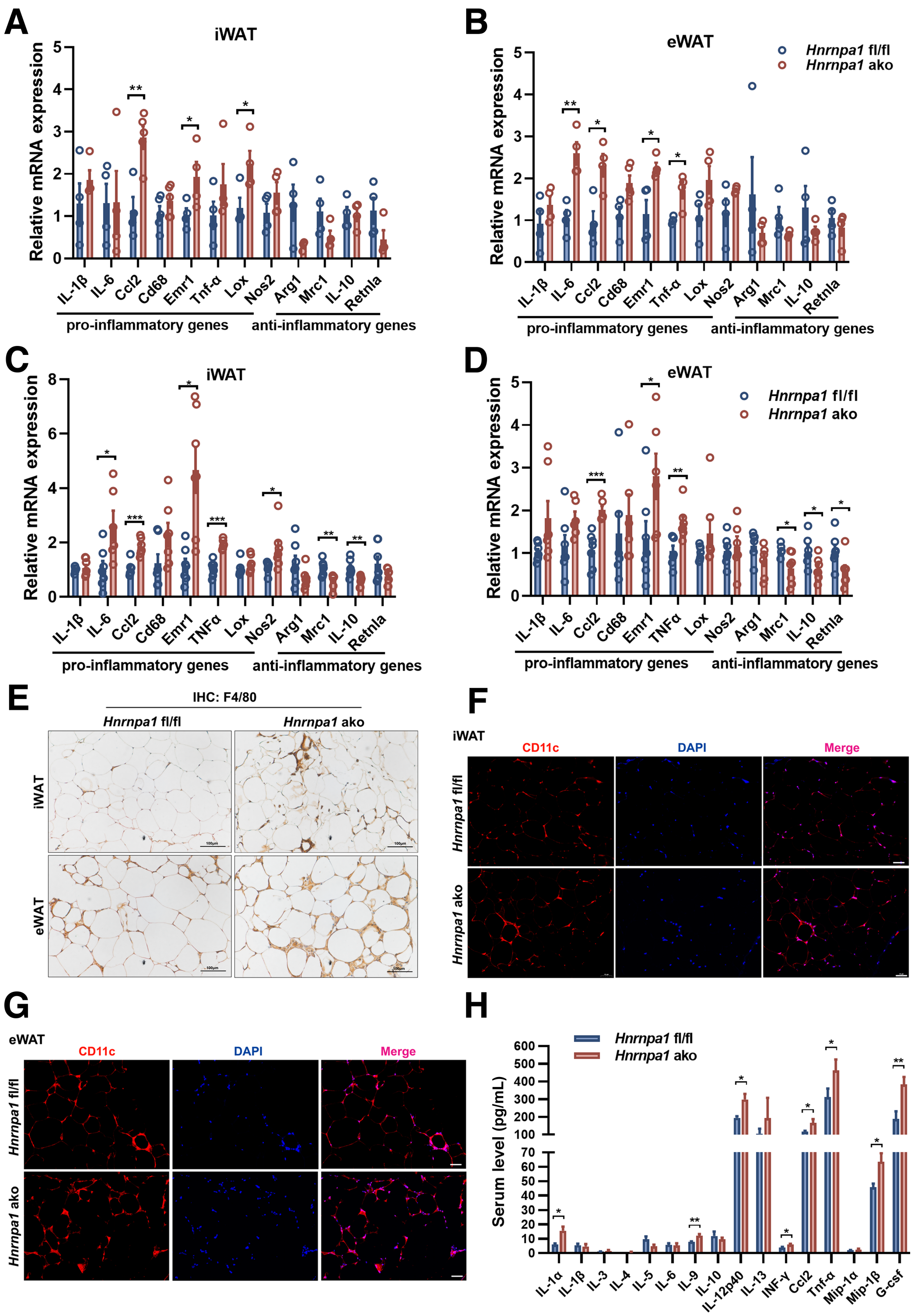

Figure 4—HNRNPA1 deficiency exacerbates adipose inflammation. *A* and *B*: RT-qPCR analysis indicating mRNA abundance of proinflammatory and anti-inflammatory genes in iWAT and eWAT under NCD feeding (n = 4 biologically independent mice per group). Male *Hnrnpa1* fl/fl and age-matched *Hnrnpa1* ako littermates then were fed an HFD for 20 weeks, and HFD feeding started at 8 weeks of age. *C* and *D*: RT-qPCR analysis indicating mRNA abundance of proinflammatory and anti-inflammatory genes in iWAT and eWAT (n = 6 biologically independent mice). *E*: Immunohistochemical (IHC) staining of F4/80 in iWAT and eWAT from *Hnrnpa1* fl/fl and *Hnrnpa1* ako mice (n = 3 biologically independent sample; scale bars = 100 μm). *F* and *G*: Representative images of immunofluorescence staining of iWAT and eWAT from 20-week HFD-fed *Hnrnpa1* fl/fl and *Hnrnpa1* ako mice (n = 3 biologically independent samples; scale bars = 50 μm). *H*: Serum inflammatory factor level analysis, including IL-1α, IL-1β, IL-3, IL-4, IL-5, IL-6, IL-9, IL-10, IL-12p40, IL-13, IFN-γ, CCL2, TNF-α, MIP-1α, MIP-1β, and granulocyte colony-stimulating factor (G-CSF). *P* values were determined by unpaired two-tailed Student *t* test (*A*–*D*, *H*). *$P < 0.05$, **$P < 0.01$, ***$P < 0.001$.

disorders of *Hnrnpa1* ako mice under HFD feeding. INCB3344 was developed as a selective small-molecule antagonist of CCR2, and several studies have identified its protective roles in inflammatory disorders (31,32). We treated 16-week DIO *Hnrnpa1* fl/fl and *Hnrnpa1* ako mice with daily subcutaneous injection of INCB3344 (30 mg/kg) for 14 days (Fig. 7*A*). At the

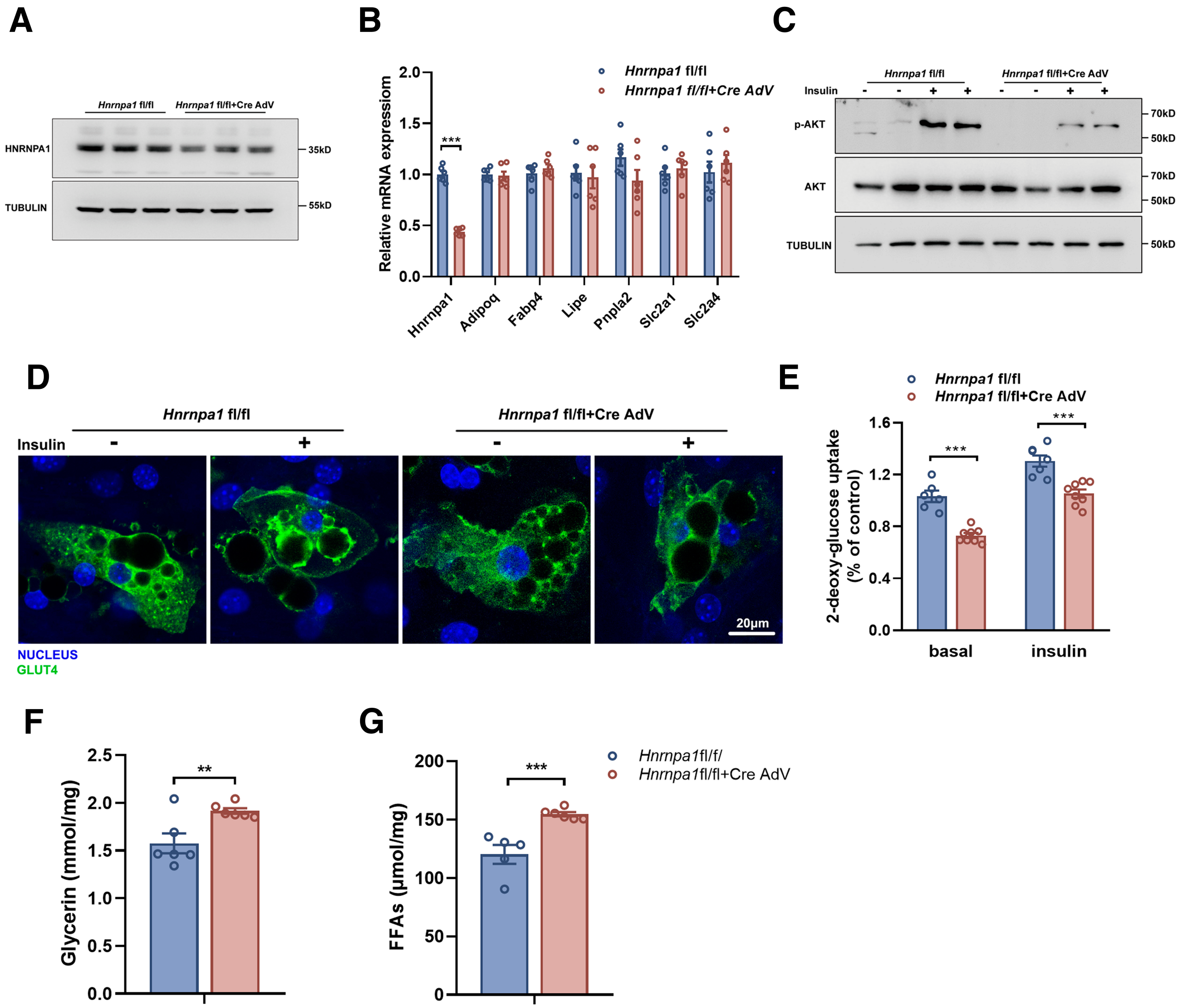

Figure 5—HNRNPA1 knockdown leads to adipocyte dysfunction. Primary iWAT preadipocytes were isolated from *Hnrnpa1* fl/fl mice and differentiated into white adipocytes. On differentiation day 3, vector adenovirus and Cre AdV were respectively infected with cultured adipocytes isolated from *Hnrnpa1* fl/fl mice to the knockout *Hnrnpa1* allele. *A*: Western blot analysis of the knockdown efficiency of HNRNPA1. *B*: RT-qPCR analysis of mRNA levels of *Hnrnpa1*, genes involved in adipogenesis (*Adipoq*, *Fabp4*), lipolysis (*Lipe*, *Pnpla2*), and glucose metabolism (*Slc2a1*, *Slc2a4*) in primary white adipocytes infected with control or Cre AdV. *C*: Western blot analysis of AKT phosphorylation in primary adipocytes after insulin (10 nmol/L) or PBS treatment. *D*: Representative images (n = 4 biologically samples per group) of membrane localization of GLUT4 in primary adipocytes after treatment with 100 nmol/L insulin or PBS for 24 h (scale bar = 20 μm). *E*: 2-Deoxy-glucose uptake in control and *Hnrnpa1* knockdown primary adipocytes with or without insulin treatment (100 nmol/L, 30 min) (n = 6 biologically independent sample per group). *F*: Adipocyte supernatant glycerin levels of control and *Hnrnpa1* knockdown primary adipocytes. *G*: Free fatty acid (FFA) levels of adipocyte supernatant from control and *Hnrnpa1* knockdown primary adipocytes. Data are mean ± SEM. *P* values were determined by unpaired two-tailed Student *t* test (*B*, *E*–*G*). $^{**}P < 0.01$, $^{***}P < 0.001$.

end of the treatment period, body and tissue weight showed no significant difference between *Hnrnpa1* fl/fl and *Hnrnpa1* ako mice with or without INCB3344 injection (Supplementary Fig. 9*A* and *B*). Remarkably, the numbers of infiltrated ATMs decreased in iWAT and eWAT when treated with INCB3344 (Fig. 7*B*). Consistently, the reduction of CD11c intensity in iWAT and eWAT was also determined in INCB3344-injected mice (Fig. 7*C* and *D* and Supplementary Fig. 10), demonstrating that INCB3344 could abolish the proinflammatory effect of HNRNPA1 deficiency. We assessed the overall state of glucose metabolism, and the results showed that INCB3344 rescued the glucose metabolic abnormalities and had a tendency to improve insulin sensitivity in adipocyte-specific knockout of HNRNPA1 (Fig. 7*E* and *F*). Collectively, our data further suggest that the obesity-related metabolic disorders of *Hnrnpa1* ako mice are mainly mediated by CCL2.

Human Adipose Tissue HNRNPA1 Is Correlated With Metabolic Traits

To further explore whether HNRNPA1 is correlated with human clinical characteristics, we analyzed its expression in paired SAT and VAT of individuals undergoing either

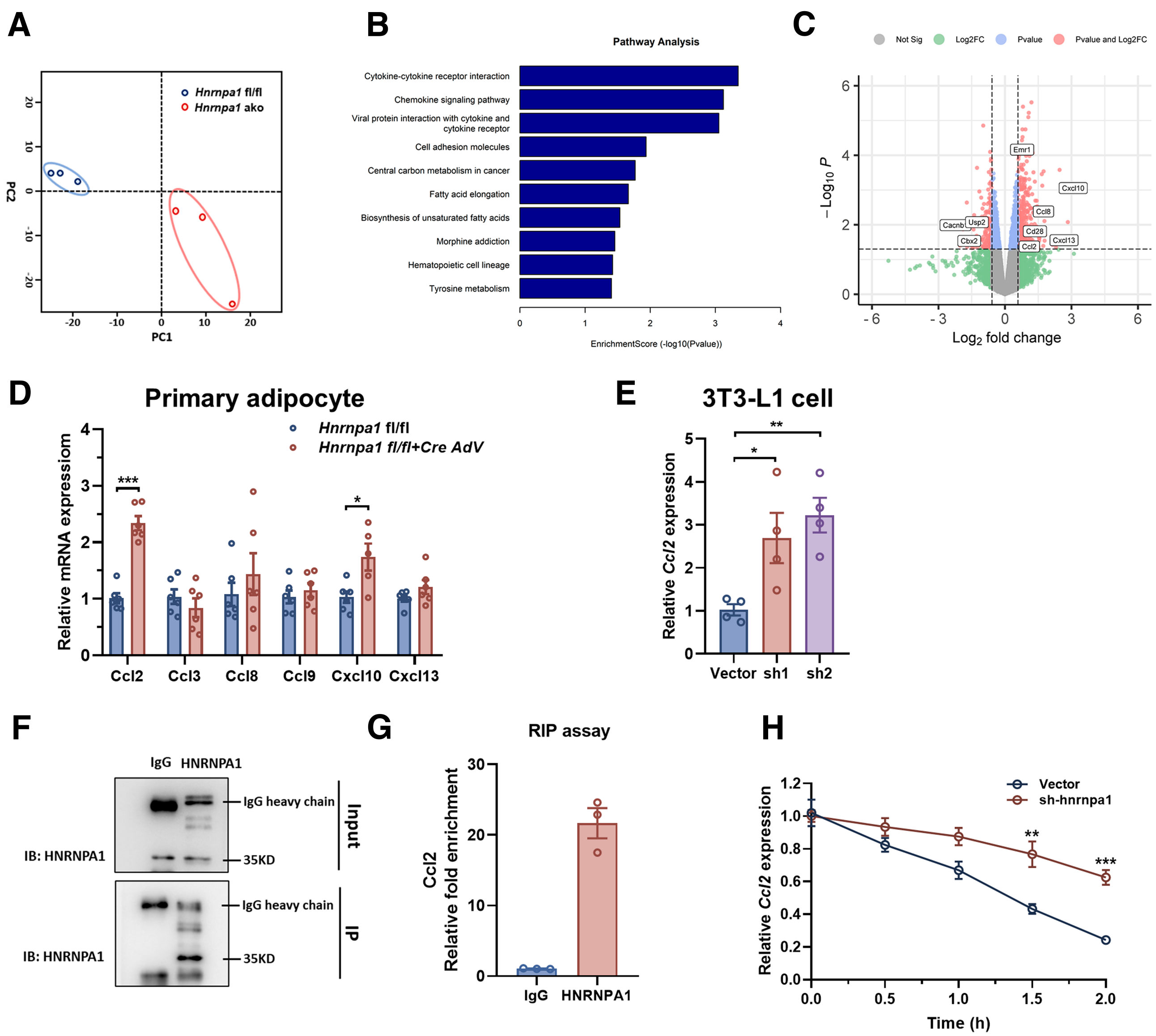

Figure 6—HNRNPA1 regulates the mRNA stability of CCL2. Male *Hnrnpa1* fl/fl and age-matched *Hnrnpa1* ako mice were fed an HFD for 20 weeks, and HFD feeding started at 8 weeks of age. *A*: Principal component (PC) analysis based on RNA-seq data from iWAT of *Hnrnpa1* fl/fl and *Hnrnpa1* ako mice (n = 3 replicates per condition). *B*: Pathway analysis of RNA-seq data from iWAT. *C*: Upregulated and downregulated genes in iWAT of *Hnrnpa1* fl/fl and *Hnrnpa1* ako mice. Data are represented in a volcano plot with fold changes ($\log_2$FC) and adjusted P values ($-\log_{10}$). *D*: RT-qPCR analysis of inflammatory chemokine genes expression (*Ccl2*, *Ccl3*, *Ccl8*, *Ccl9*, *Cxcl10*, and *Cxcl13*) in primary white adipocytes isolated from *Hnrnpa1* fl/fl mice infected with control or Cre AdV. *E*: RT-qPCR analysis of *Ccl2* expression of 3T3-L1 cells infected with lentiviral vector or two different shRNA target clones (*Hnrnpa1* sh1, *Hnrnpa1* sh2). *F* and *G*: RIP assay assessing HNRNPA1 binding with Ccl2 in 3T3-L1 adipocytes (n = 3). *H*: mRNA level of *Ccl2* in control or HNRNPA1 knockdown 3T3-L1 adipocytes upon transcriptional inhibition with actinomycin D at the indicated times (n = 4). P values were determined by unpaired two-tailed Student t test (*D*, *E*, and *G*) or multiple t tests (*H*). *$P < 0.05$, **$P < 0.01$, ***$P < 0.001$. IB, immunoblotting; IP, immunoprecipitation; Not Sig, not significant.

elective abdominal surgery for cholecystectomy or weight reduction bariatric surgery. The clinical characteristics are shown in Supplementary Table 4. We observed a negative correlation of HNRNPA1 expression with BMI, fat percentage, and subcutaneous fat area in SAT (Fig. 8*A*–*C*). Notably, *LEP* gene expression was significantly correlated with HNRNPA1 expression (Fig. 8*D*). Among individuals with detectable HNRNPA1 expression, 33 were followed up 1 year after bariatric surgery. The percentage of total weight loss (TWL%) is an accurate indicator to assess efficiency of weight loss surgery (33). We found that a higher level of HNRNPA1 correlated with better TWL% (Fig. 8*E*), indicating that HNRNPA1 expression in SAT might predict the outcome of bariatric surgery (as illustrated in Fig. 8*F*).

DISCUSSION

In the current study, we demonstrate HNRNPA1 as a regulator that links adipose tissue inflammation to metabolic dysfunction. *Hnrnpa1* ako mice were generated and used

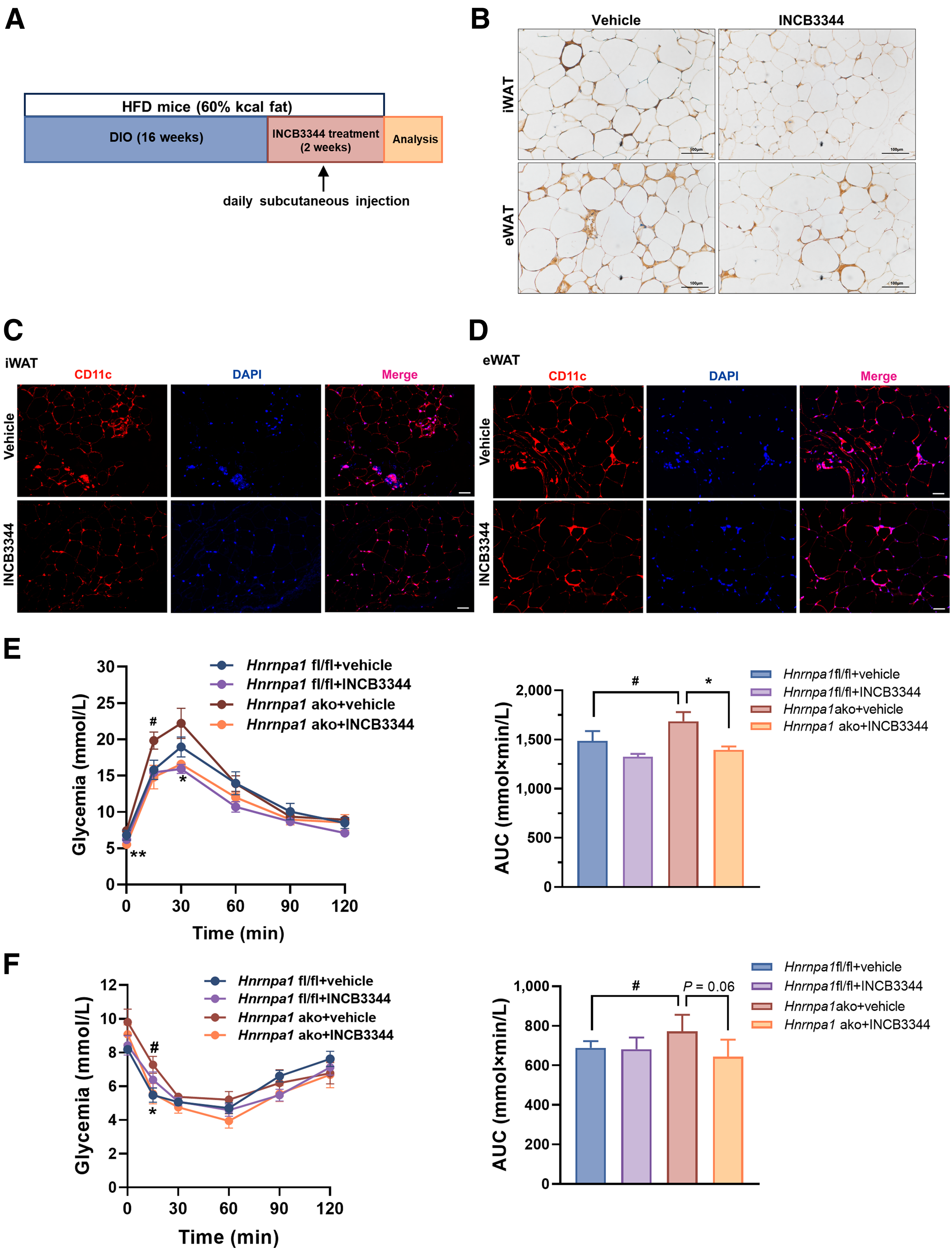

Figure 7—CCL2-CCR2 antagonist improves metabolic disorder of *Hnrnpa1* ako mice under HFD feeding. Male *Hnrnpa1* fl/fl and age-matched *Hnrnpa1* ako mice were fed an HFD for 16 weeks, and HFD feeding started at 8 weeks of age. *A*: Overview of INCB344 injection (2 weeks) in mice fed an HFD at the start of the experiment. *B*: Immunohistochemical staining of F4/80 in iWAT and eWAT from *Hnrnpa1* fl/fl and *Hnrnpa1* ako mice, with or without 2 weeks of INCB3344 injection (n = 3 biologically independent samples per group; scale bars = 100 μm). *C* and *D*: Representative images of immunofluorescence staining of iWAT and eWAT of *Hnrnpa1* fl/fl and *Hnrnpa1* ako mice, with or without 2 weeks of INCB3344 injection (n = 3 biologically independent samples; scale bars = 50 μm). *E*: Glucose tolerance test and area under the curve

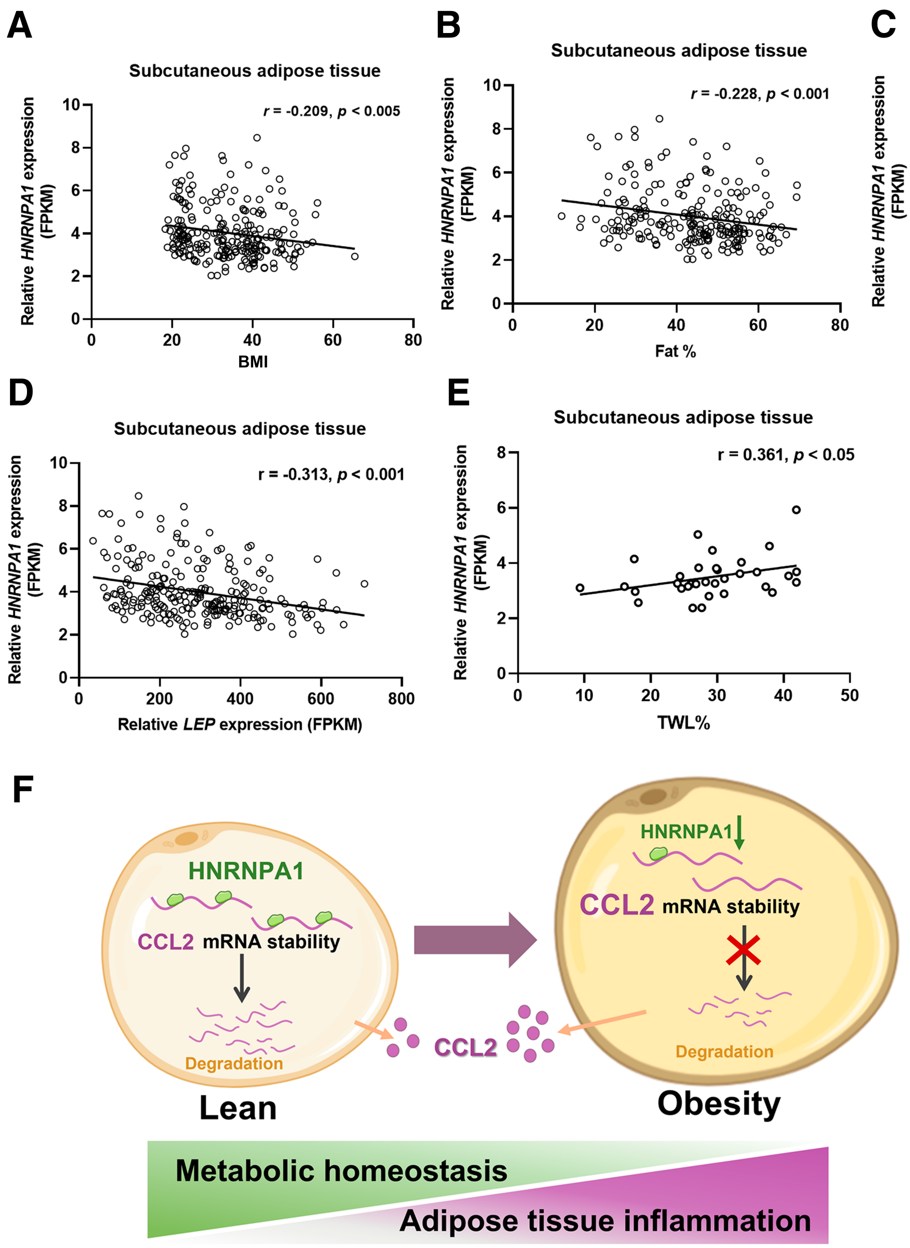

Figure 8—Human adipose tissue HNRNPA1 expression is correlated with obesity and metabolic traits. *A–C*: The relationship between *HNRNPA1* expression and BMI, fat percentage, and subcutaneous fat area (SFA) in SAT. *D*: The relationship between *HNRNPA1* and *LEP* expression. *E*: The relationship between baseline *HNRNPA1* expression and TWL% in individuals 1 year after metabolic surgery. *F*: Model of how adipocyte HNRNPA1 regulates CCL2 expression and thus influences adipose tissue inflammation and metabolic balance. Spearman correlation analysis is shown by *r* values and two-tailed *P* values. FPKM, fragments per kilobase of transcript per million mapped reads.

in metabolic studies to clarify the role of HNRNPA1 in insulin sensitivity, glucose tolerance, and hepatic glucose and lipid metabolism, as well as adipose tissue inflammation. Cell experiments revealed that HNRNPA1 knockdown led to adipocyte dysfunction. Mechanistically, HNRNPA1 regulated the mRNA stability of chemokine CCL2, which influenced the recruitment and activation of ATMs. Moreover, HNRNPA1 expression in human WAT was negatively correlated with indicators of fat accumulation and indicated the outcome of metabolic surgery.

Previous studies have reported that HNRNPA1 is involved in metabolic regulation. An earlier study found that HNRNPA1 was one of the RNA-processing genes with decreased expression in human liver and muscle samples

(AUC) (n = 7 biologically independent mice per group). *F*: Insulin tolerance test and AUC (n = 7 biologically independent mice per group). Data are mean ± SEM. *P* values were determined by two-way ANOVA with Šidák multiple comparisons test (*E* and *F*). *$P < 0.05$, comparing *Hnrnpa1* ako with vehicle; #$P < 0.05$, comparing *Hnrnpa1* fl/fl with vehicle. DIO, diet-induced obesity.

(34). Hepatic HNRNPA1 overexpression could relieve hyperglycemia and liver steatosis from HFD feeding by binding and regulating calmodulin mRNAs (17). Studies in skeletal muscle showed that HNRNPA1 improves insulin resistance via regulating mRNA expression of CPT1b (18) or glycogen synthase 1 (26). The metabolic protective roles in the liver and muscle prompted us to explore the potential function of HNRNPA1 in adipose tissue. Although it was identified that loss of HNRNPA1 in murine skeletal muscle exacerbated HFD-induced insulin resistance and hepatic steatosis (26), we revealed the new role of HNRNPA1 in adipocytes via an entirely different inflammatory mechanism, emphasizing the contribution of adipocyte HNRNPA1 to systemic metabolism.

Apart from regulating alternative mRNA splicing by binding mRNA elements, HNRNPA1 also plays important roles via regulating mRNA stability (15). HNRNPA1 could bind with adenylate uridylate–rich sequences to modulate mRNA stability of IL-2 (35) and granulocyte-macrophage colony-stimulating factor, which maintains the function of T cells (36). In addition, HNRNPA1 could affect cellular senescence and apoptosis via regulating cIAP1 mRNA stability (37). Recent studies revealed that HNRNPA1 exerts antiaging effects in human lung fibroblast and vascular cells via regulating the degradation of SIRT1 or octamer-binding transcriptional factor 4 (38,39). Our study initially identified a downregulation of HNRNPA1 expression in obesity. A previous study reported a decrease in HNRNPA1 following insulin treatment (26), which suggested that chronic hyperinsulinemia may regulate the expression of HNRNPA1. This further highlighted the close relationship between HNRNPA1 and metabolism. Then, we identified that adipocyte HNRNPA1 deficiency disturbed the metabolic homeostasis in both in vivo and in vitro experiments. Considering that HNRNPA1 is a vital posttranscriptional regulator, we speculate that HNRNPA1 might function by regulating mRNA stability in adipose tissues.

Notably, proinflammatory factor CCL2 was hypothesized to be a linker between HNRNPA1 depletion and adipose tissue proinflammatory response in this study. CCL2 is secreted not only by macrophages and endothelial cells but also by adipocytes (40). It is well established that CCL2 mediates macrophage recruitment and activation (41). HFD-induced and *ob/ob* obese mice had high expression levels of CCL2 in WAT, which has been extended to humans (42). AP2 promoter–mediated *Ccl2* transgene mice exhibited ATM infiltration, insulin resistance, and hepatic steatosis under HFD feeding (40). Furthermore, CCL2 or CCR2 homozygous knockout mice showed improved inflammation and metabolic dysfunction (43). These studies identified the connection among CCL2, adipose tissue inflammation, and metabolic system disorders. Although the research on adipose tissue inflammation began earlier, emerging research continued to reveal its new mechanism and clinical significance (44). In our sequencing data of iWAT in *Hnrnpa1* ako mice, the most noticeable changes were cytokine-cytokine receptor interaction and chemokine pathway. Increased CCL2 expression was identified in adipose tissue, primary differentiated adipocytes, and 3T3-L1 cells. Thus, we reveal a new regulatory mechanism of ATM infiltration through the HNRNPA1-CCL2 axis. Besides, the function of adipocyte secretion on systemic inflammation has also been continuously explored (45,46). Apart from its role in recruiting immune cells at the tissue level, previous studies found that CCL2 could directly regulate the function of adipocytes (42), pancreatic islet cells (47), skeletal muscle cells (48), and tubular epithelial cells (49) independent of CCR2. So, impaired adipocyte function may be due to the autocrine regulatory role of CCL2. This study clarifies the regulation and function of CCL2 derived from adipocytes.

Given the important roles of CCL2, previous studies examined its regulatory mechanisms. It can be transcriptionally induced by inflammatory stimuli (50), platelet-derived growth factor (51), and the mTORC1-FOXK1 axis (52). Furthermore, posttranscriptional regulation plays a crucial role in CCL2 expression. It was identified that oxygen radicals and pyroglutamate enhance CCL2 mRNA transcript stability (53). The glucocorticoid receptor bound directly to the three stem-loops in the 5′ end of CCL2 and destabilized its mRNA, implicating a role in immune responses (54). Platelet-derived growth factor, angiotensin II (55), prostaglandin E receptor subtype 2 signaling (56), and ribosomal protein L22 (57) were also reported to function in stabilizing or degrading CCL2 mRNA. Recently, Xiao et al. (58) reported that tristetraprolin decreased CCL2 mRNA stability by regulating m6A methylation to ameliorate hepatic injury. Parajuli et al. (59) showed that AT-rich interaction domain-containing protein 5a stabilized CCL2 mRNA to regulate the tumor microenvironment. Therefore, as a vital chemokine in adipose tissue and a potential therapeutic target, our findings provide evidence that HNRNPA1 interacts directly with CCL2 and regulates its mRNA stability in differentiated adipocytes.

In concordance with that study based on *Ccl2* transgenic mice, *Hnrnpa1* ako mice showed a similar phenotype when maintained on an HFD, including impaired glucose tolerance and insulin sensitivity, accumulated ATM infiltration, and aggravated hepatic steatosis under HFD feeding, while the body weight, adipose tissue weight, and food intake showed no change in *Hnrnpa1* ako mice. We also show that administration of CCL2-CCR2 signaling inhibitor to obese mice inhibited the ATM infiltration and partly improved glucose homeostasis. All our results highlight that adipocyte HNRNPA1 functions via chemokine CCL2.

A limitation of our study is that we could not define whether CCL2 is the only target that mediates the effect of HNRNPA1 on adipose tissue inflammation. Given the differentially expressed genes revealed by sequencing results, it is conceivable that HNRNPA1 may have other as-yet undiscovered target genes in adipocytes. Additionally, double adipocyte-specific *Hnrnpa1/Ccl2* knockout mice would likely be the optimal choice to demonstrate the role of HNRNPA1 acting through CCL2 in adipocytes. Besides, the underlying mechanism needs to be investigated in further studies, since the specific binding site in CCL2 was not elucidated. Unraveling in-depth mechanisms involved in HNRNPA1-regulated inflammation in adipocytes will therefore be the focus of future studies.

In summary, we report that HNRNPA1 was downregulated in WAT of obese individuals and correlated with clinical indicators. The reduced HNRNPA1 inhibited CCL2 mRNA degradation, leading to ATM infiltration, which activated inflammation and metabolic dysfunction. Our data unravel a balance between HNRNPA1-CCL2 and adipose tissue inflammation, which is disturbed in obesity. Further studies are needed to understand the comprehensive mechanism and its potential therapeutic impact.

Acknowledgments. The authors thank Dr. Jiangfeng Ke (People's Hospital of Fujian University of Traditional Chinese Medicine) for providing adipoq-Cre transgenic mice.

Funding. This research was supported by National Natural Science Foundation of China grants 82200897 and 82170889 and Shanghai Research Center for Endocrine and Metabolic Diseases grant 2022ZZ01002.

Duality of Interest. No potential conflicts of interest relevant to this article were reported.

Author Contributions. X. Li, Y.S., and Y.X. performed experiments. X. Li, X. Lu, J.S., and W.L. interpreted data. X. Li, Y.Y., and Y.B. conceived the idea and developed the study design. X. Li wrote the manuscript. T.H., J.Z., and X.M. analyzed the RNA-seq and clinical data. Y.Y. and Y.B. are the guarantors of this work and, as such, had full access to all the data in the study and take responsibility for the integrity of the data and the accuracy of the data analysis.

References

1. Blüher M. Obesity: global epidemiology and pathogenesis. Nat Rev Endocrinol 2019;15:288–298
2. Chavakis T, Alexaki VI, Ferrante AW Jr. Macrophage function in adipose tissue homeostasis and metabolic inflammation. Nat Immunol 2023;24:757–766
3. Sakers A, De Siqueira MK, Seale P, Villanueva CJ. Adipose-tissue plasticity in health and disease. Cell 2022;185:419–446
4. Scheja L, Heeren J. The endocrine function of adipose tissues in health and cardiometabolic disease. Nat Rev Endocrinol 2019;15:507–524
5. Fasshauer M, Blüher M. Adipokines in health and disease. Trends Pharmacol Sci 2015;36:461–470
6. Ouchi N, Parker JL, Lugus JJ, Walsh K. Adipokines in inflammation and metabolic disease. Nat Rev Immunol 2011;11:85–97
7. Agudelo LZ, Ferreira DMS, Cervenka I, et al. Kynurenic acid and Gpr35 regulate adipose tissue energy homeostasis and inflammation. Cell Metab 2018;27:378–392.e5
8. Yan J, Zhang Y, Yu H, et al. GPSM1 impairs metabolic homeostasis by controlling a pro-inflammatory pathway in macrophages. Nat Commun 2022; 13:7260
9. Reilly SM, Saltiel AR. Adapting to obesity with adipose tissue inflammation. Nat Rev Endocrinol 2017;13:633–643
10. Gerstberger S, Hafner M, Tuschl T. A census of human RNA-binding proteins. Nat Rev Genet 2014;15:829–845
11. Siang DTC, Lim YC, Kyaw AMM, et al. The RNA-binding protein HuR is a negative regulator in adipogenesis. Nat Commun 2020;11:213
12. Li J, Gong L, Liu S, et al. Adipose HuR protects against diet-induced obesity and insulin resistance. Nat Commun 2019;10:2375
13. Li Y, Wang D, Ping X, et al. Local hyperthermia therapy induces browning of white fat and treats obesity. Cell 2022;185:949–966.e19
14. He Y, Smith R. Nuclear functions of heterogeneous nuclear ribonucleoproteins A/B. Cell Mol Life Sci 2009;66:1239–1256
15. Jean-Philippe J, Paz S, Caputi M. hnRNP A1: the Swiss army knife of gene expression. Int J Mol Sci 2013;14:18999–19024
16. Koo JH, Lee HJ, Kim W, Kim SG. Endoplasmic reticulum stress in hepatic stellate cells promotes liver fibrosis via PERK-mediated degradation of HNRNPA1 and up-regulation of SMAD2. Gastroenterology 2016;150:181–193.e8
17. Wang J, Yang W, Chen Z, et al. Long noncoding RNA lncSHGL recruits hnRNPA1 to suppress hepatic gluconeogenesis and lipogenesis. Diabetes 2018;67:581–593
18. Gui W, Zhu WF, Zhu Y, et al. LncRNAH19 improves insulin resistance in skeletal muscle by regulating heterogeneous nuclear ribonucleoprotein A1. Cell Commun Signal 2020;18:173
19. Li X, Zhang H, Ma X, et al. FSTL3 is highly expressed in adipose tissue of individuals with overweight or obesity and is associated with inflammation. Obesity (Silver Spring) 2023;31:171–183
20. Carithers LJ, Moore HM. The Genotype-Tissue Expression (GTEx) Project. Biopreserv Biobank 2015;13:307–308
21. Poitou C, Perret C, Mathieu F, et al. Bariatric surgery induces disruption in inflammatory signaling pathways mediated by immune cells in adipose tissue: a RNA-seq study. PLoS One 2015;10:e0125718
22. Grabner GF, Xie H, Schweiger M, Zechner R. Lipolysis: cellular mechanisms for lipid mobilization from fat stores. Nat Metab 2021;3:1445–1465
23. Kratz M, Coats BR, Hisert KB, et al. Metabolic dysfunction drives a mechanistically distinct proinflammatory phenotype in adipose tissue macrophages. Cell Metab 2014;20:614–625
24. Li P, Lu M, Nguyen MTA, et al. Functional heterogeneity of CD11c-positive adipose tissue macrophages in diet-induced obese mice. J Biol Chem 2010;285:15333–15345
25. Marcelin G, Silveira ALM, Martins LB, Ferreira AV, Clément K. Deciphering the cellular interplays underlying obesity-induced adipose tissue fibrosis. J Clin Invest 2019;129:4032–4040
26. Zhao M, Shen L, Ouyang Z, et al. Loss of hnRNP A1 in murine skeletal muscle exacerbates high-fat diet-induced onset of insulin resistance and hepatic steatosis. J Mol Cell Biol 2020;12:277–290
27. Huang S, Czech MP. The GLUT4 glucose transporter. Cell Metab 2007;5:237–252
28. Dommel S, Blüher M. Does C-C motif chemokine ligand 2 (CCL2) link obesity to a pro-inflammatory state? Int J Mol Sci 2021;22:1500
29. Kang YS, Lee MH, Song HK, et al. CCR2 antagonism improves insulin resistance, lipid metabolism, and diabetic nephropathy in type 2 diabetic mice. Kidney Int 2010;78:883–894
30. Cheng J, Yang Z, Ge XY, et al. Autonomous sensing of the insulin peptide by an olfactory G protein-coupled receptor modulates glucose metabolism. Cell Metab 2022;34:240–255.e10
31. Brodmerkel CM, Huber R, Covington M, et al. Discovery and pharmacological characterization of a novel rodent-active CCR2 antagonist, INCB3344. J Immunol 2005;175:5370–5378
32. Tan X, Hu L, Shu Z, et al. Role of CCR2 in the development of streptozotocin-treated diabetic cardiomyopathy. Diabetes 2019;68:2063–2073
33. Hatoum IJ, Kaplan LM. Advantages of percent weight loss as a method of reporting weight loss after Roux-en-Y gastric bypass. Obesity (Silver Spring) 2013;21:1519–1525
34. Pihlajamäki J, Lerin C, Itkonen P, et al. Expression of the splicing factor gene SFRS10 is reduced in human obesity and contributes to enhanced lipogenesis. Cell Metab 2011;14:208–218
35. Henics T, Sanfridson A, Hamilton BJ, Nagy E, Rigby WF. Enhanced stability of interleukin-2 mRNA in MLA 144 cells. Possible role of cytoplasmic AU-rich sequence-binding proteins. J Biol Chem 1994;269:5377–5383
36. Hamilton BJ, Burns CM, Nichols RC, Rigby WF. Modulation of AUUUA response element binding by heterogeneous nuclear ribonucleoprotein A1 in

human T lymphocytes. The roles of cytoplasmic location, transcription, and phosphorylation. J Biol Chem 1997;272:28732–28741

37. Zhao TT, Graber TE, Jordan LE, et al. hnRNP A1 regulates UV-induced NF-kappaB signalling through destabilization of cIAP1 mRNA. Cell Death Differ 2009;16:244–252

38. Wang H, Han L, Zhao G, et al. hnRNP A1 antagonizes cellular senescence and senescence-associated secretory phenotype via regulation of SIRT1 mRNA stability. Aging Cell 2016;15:1063–1073

39. Han YM, Bedarida T, Ding Y, et al. β-Hydroxybutyrate prevents vascular senescence through hnRNP A1-mediated upregulation of Oct4. Mol Cell 2018;71:1064–1078.e5

40. Kanda H, Tateya S, Tamori Y, et al. MCP-1 contributes to macrophage infiltration into adipose tissue, insulin resistance, and hepatic steatosis in obesity. J Clin Invest 2006;116:1494–1505

41. Lu B, Rutledge BJ, Gu L, et al. Abnormalities in monocyte recruitment and cytokine expression in monocyte chemoattractant protein 1-deficient mice. J Exp Med 1998;187:601–608

42. Sartipy P, Loskutoff DJ. Monocyte chemoattractant protein 1 in obesity and insulin resistance. Proc Natl Acad Sci U S A 2003;100:7265–7270

43. Weisberg SP, Hunter D, Huber R, et al. CCR2 modulates inflammatory and metabolic effects of high-fat feeding. J Clin Invest 2006;116:115–124

44. Unamuno X, Gómez-Ambrosi J, Ramírez B, et al. NLRP3 inflammasome blockade reduces adipose tissue inflammation and extracellular matrix remodeling. Cell Mol Immunol 2021;18:1045–1057

45. Han CY, Kang I, Harten IA, et al. Adipocyte-derived versican and macrophage-derived biglycan control adipose tissue inflammation in obesity. Cell Rep 2020;31:107818

46. Maqdasy S, Lecoutre S, Renzi G, et al. Impaired phosphocreatine metabolism in white adipocytes promotes inflammation. Nat Metab 2022;4: 190–202

47. Cai K, Qi D, Hou X, et al. MCP-1 upregulates amylin expression in murine pancreatic β cells through ERK/JNK-AP1 and NF-κB related signaling pathways independent of CCR2. PLoS One 2011;6:e19559

48. Viedt C, Vogel J, Athanasiou T, et al. Monocyte chemoattractant protein-1 induces proliferation and interleukin-6 production in human smooth muscle cells by differential activation of nuclear factor-kappaB and activator protein-1. Arterioscler Thromb Vasc Biol 2002;22:914–920

49. Viedt C, Dechend R, Fei J, Hänsch GM, Kreuzer J, Orth SR. MCP-1 induces inflammatory activation of human tubular epithelial cells: involvement of the transcription factors, nuclear factor-kappaB and activating protein-1. J Am Soc Nephrol 2002;13:1534–1547

50. Gschwandtner M, Derler R, Midwood KS. More than just attractive: how CCL2 influences myeloid cell behavior beyond chemotaxis. Front Immunol 2019;10:2759

51. Cochran BH, Reffel AC, Stiles CD. Molecular cloning of gene sequences regulated by platelet-derived growth factor. Cell 1983;33:939–947

52. Nakatsumi H, Matsumoto M, Nakayama KI. Noncanonical pathway for regulation of CCL2 expression by an mTORC1-FOXK1 axis promotes recruitment of tumor-associated macrophages. Cell Rep 2017;21:2471–2486

53. Cynis H, Hoffmann T, Friedrich D, et al. The isoenzyme of glutaminyl cyclase is an important regulator of monocyte infiltration under inflammatory conditions. EMBO Mol Med 2011;3:545–558

54. Park OH, Park J, Yu M, An HT, Ko J, Kim YK. Identification and molecular characterization of cellular factors required for glucocorticoid receptor-mediated mRNA decay. Genes Dev 2016;30:2093–2105

55. Liu B, Dhawan L, Blaxall BC, Taubman MB. Protein kinase Cδ mediates MCP-1 mRNA stabilization in vascular smooth muscle cells. Mol Cell Biochem 2010;344:73–79

56. Aoki T, Frösen J, Fukuda M, et al. Prostaglandin E2-EP2-NF-κB signaling in macrophages as a potential therapeutic target for intracranial aneurysms. Sci Signal 2017;10:eaah6037

57. Das AS, Basu A, Kumar R, et al. Post-transcriptional regulation of C-C motif chemokine ligand 2 expression by ribosomal protein L22 during LPS-mediated inflammation. FEBS J 2020;287:3794–3813

58. Xiao P, Li M, Zhou M, et al. TTP protects against acute liver failure by regulating CCL2 and CCL5 through m6A RNA methylation. JCI Insight 2021;6:e149276

59. Parajuli G, Tekguc M, Wing JB, et al. Arid5a promotes immune evasion by augmenting tryptophan metabolism and chemokine expression. Cancer Immunol Res 2021;9:862–876